Real-Time Hybrid Particle Swarm and Grey Wolf Optimization for PV Curtailment Reduction and Battery Longevity in Isolated PV-Battery Microgrids

KATHI AVINASH
Department of Electrical & Electronics Engineering
Vignan's Institute of Information Technology, India
avinash.k@vignaniit.edu.in

Raghavendra P
Department of Electrical & Electronics Engineering
Ballari institute of technology and management, Ballari
raghudts@gmail.com

Ahmed Ali
Department of Electrical and Electronic Engineering Technology
University of Johannesburg
Johannesburg, SOUTH AFRICA
aali@uj.ac.za

***Abstract*— Rule-based voltage threshold controllers are the default for isolated PV-battery microgrids — simple to implement but wasteful in practice, with curtailment rates that can exceed 20% of installed capacity. This paper proposes a hybrid PSO-GWO algorithm that combines Particle Swarm Optimization's rapid global exploration (iterations 1–50) with Grey Wolf Optimizer's systematic exploitation (iterations 51–100) in a two-phase architecture designed to overcome the premature convergence that limits standalone metaheuristics. The hybrid was evaluated on 277 days of real operational data (324,795 one-minute records) from an isolated photovoltaic-battery microgrid in Réunion Island's Mafate region and benchmarked against standalone PSO, GA, and GWO under identical conditions. PSO-GWO reduced PV curtailment by 99.85% — from 1,423.37 kWh to just 2.08 kWh — cut battery stress by 81.66%, and generated 22 Pareto-optimal solutions covering the full trade-off space between energy efficiency, supply reliability, and battery longevity. Computation time was 1.73 seconds per 60-minute optimization cycle, confirming real-time deployment feasibility. The recovered generation amounts to 248 MWh annually, with 40% battery life extension deferring €4,800 in replacement costs per system.**

I. INTRODUCTION

1.1 Motivation and Background

Isolated PV-battery microgrids serving remote island communities run into a control problem that mainland grids never face — when the battery is full and generation keeps coming, the only option is to waste it. Curtailment rates above 20% of installed PV capacity are common under rule-based voltage threshold controllers, which make charge/discharge decisions based on a single SOC reading with no awareness of what comes next [1], [2]. At the same time, supply deficits during evening peaks and cloud transients put battery cycling under stress, and in a location where replacement means helicopter logistics, battery longevity is as important as energy delivery.

The analysis to minimise curtailment, avoid deficits and protect the battery pulls us in different directions. This charge strategy is aggressive, which results in less curtailment but where the battery cycles hard. A more conservative approach shields the battery but loses generation. This trade-off cannot be done sensibly with rule-based systems because they have no ability to search through time or optimize for multiple goals at once. However, both require some sort of optimization metaheuristic. This paper combines them in a two-phase structure and tests it on 277 days of real operational data.

1.2 Literature Review

The energy management of the first type of microgrids were based on linearised battery models (predictive) and simplified photovoltaic forecasts to make them tractable — slow and rigid for a sub-minute response time on an island solution. This is why metaheuristic approaches became a viable alternative, performing derivative-free search over non-convex landscapes with multiple objectives without the need for convex formulation. Improved versions of traditional algorithms have shown performance gains as well: multi-objective moth flame algorithms reduce emissions and voltage deviations by 60–86% [3], and a hybrid golden search algorithm has displayed better results than standalone methods for off-grid renewable sizing [4].

Compared with other metaheuristics, PSO has been most widely used for microgrid scheduling — fast convergence and low tuning ease implementation [5]. PSO with GWO has been proposed for maximum power point tracking under partial shading [6] and also showed better performance than conventional methods in sizing a grid-independent system using an approach based on GWO alone. The two have well-established complementarity: GWO exploits better solutions through pack coordination, and PSO quickly moves to attractive regions of the space. Work has similarly advanced on battery degradation-aware optimization, finding that explicit penalties in objective functions for battery stress extend asset lifespan without significant loss in energy performance [8], [9].

The gap is straightforward: almost all published metaheuristic microgrid work tests standalone algorithms, uses simplified cycle-count battery stress metrics rather than current fluctuation rates, and does not validate execution times against the <5-second latency that operational embedded controllers actually require [10]. This paper addresses all three gaps through a hybrid PSO-GWO architecture tested on real one-minute resolution operational data with full real-time timing validation

1.3 Main Contributions

This paper makes five contributions to island microgrid energy management:

Hybrid PSO-GWO architecture: A two-phase algorithm using PSO for global exploration (iterations 1–50) then GWO for systematic exploitation (iterations 51–100). The PSO swarm initialises the GWO wolf pack directly — no re-randomisation — preserving accumulated search knowledge across the phase transition.

Battery stress formulation using current fluctuation rates: The objective function penalises |ΔI_bat| rather than cycle counts — a more accurate degradation proxy for lead-gel batteries under tropical thermal conditions where current spikes drive capacity fade more than cycle depth.

Real-time execution validation: All four algorithms (PSO, GA, GWO, PSO-GWO) are timed on 277 days of real 1-minute data with 60 decision variables per 60-minute horizon. PSO-GWO completes in 1.73 seconds — well within the <5-second latency that operational embedded controllers require.

Operational impact quantification: PSO-GWO reduces PV curtailment by 99.85% (1,423.37 → 2.08 kWh) and battery stress by 81.66% versus rule-based baseline. Annualised, this recovers 248 MWh of previously wasted generation and extends battery life by 40%, deferring €4,800 in replacement costs per system.

Analysis of Pareto front quality: hypervolume indicators and spacing metrics with a concrete set of 22 non-dominated solutions that provide operators with this as distinct trade-off strategies, rather than a solution at a single point

II. Methodology

2.1 System Architecture and Problem Formulation

The microgrid comprises a 7.0 kWp PV array, a 63 kWh lead-gel battery (46–52V operational range), and three residential loads averaging 300W. The energy management system runs at one-minute resolution over a 60-minute receding horizon, producing battery power scheduling decisions bounded at ±3.5 kW.

Three objectives are minimised simultaneously: PV curtailment C (wasted generation when the battery is full), supply deficit D (unmet demand during low-generation periods), and battery stress S (current fluctuation rate |ΔI_bat| as a degradation proxy for lead-gel chemistry). The decision vector $x \in \mathbb{R}^{60}$ specifies battery power adjustments per minute, subject to $-3.5 \leqslant x_i \leqslant 3.5$ kW and voltage-based SOC limits. System energy balance is simulated as P_net(t) = P_PV(t) + x(t) − P_load(t), with curtailment accumulating when P_net > 0 and deficit when P_net < 0.

2.2 Metaheuristic Algorithm Implementations

Four algorithms are implemented and benchmarked under identical conditions:

PSO uses 30 particles with adaptive inertia weight decreasing linearly from 0.9 to 0.4 over 100 iterations, $c_1 = c_2 = 2.0$, and v_max = 1.0 kW. Personal and global best solutions are tracked using Pareto dominance for multi-objective selection.

GA runs 30 individuals over 100 generations with tournament selection (size 3), two-point crossover (rate 0.8), and Gaussian mutation (rate 0.02, σ = 0.5 kW). The top 10% of non-dominated solutions are kept unchanged across generations.

GWO uses 30 agents over 100 iterations with alpha, beta, and delta wolves representing the three best Pareto solutions. Position updates average the three leaders' influences: x(t+1) = (X_α + X_β + X_δ)/3. The convergence parameter a decreases linearly from 2 to 0, shifting the balance from exploration to exploitation.

Hybrid PSO-GWO splits the 100-iteration budget into two phases. Iterations 1–50 run PSO for rapid global exploration. Iterations 51–100 switch to GWO for systematic refinement — the PSO swarm's final positions directly initialise the GWO wolf pack, carrying accumulated search knowledge across the phase transition without re-randomisation.

2.3 Evaluation Framework

Five metrics assess performance: objective values (curtailment, deficit, stress), Pareto front quality (hypervolume indicator, spacing metric), convergence rate (iterations to 95% of final fitness), execution time per optimization cycle, and improvement over the rule-based baseline (voltage thresholds: 52V for curtailment activation, 46V for deficit management).

The 277-day dataset (324,795 one-minute records, May 2020 – February 2021) splits into training (through December 2020), validation (January 2021), and test (February 2021). Statistical significance uses Wilcoxon signed-rank tests with $p < 0.05$ threshold for paired algorithm comparisons.

III. Mathematical Modelling

3.1 Multi-Objective Optimization Problem Formulation

The energy management problem minimises three objectives simultaneously over a 60-minute receding horizon:

The multi-objective function is defined following [1]:

$$\min_{\mathbf{x}} \mathbf{F}(\mathbf{x}) = [f_1(\mathbf{x}), f_2(\mathbf{x}), f_3(\mathbf{x})] \quad (1)$$

where f_1 is PV curtailment (kWh), f_2 is supply deficit (kWh), and f_3 is battery stress (A·min). The decision vector $x \in \mathbb{R}^{60}$ specifies battery power adjustments per minute, bounded at $-3.5 \leq x_i \leq 3.5$ kW with voltage-based SOC limits (46–52V).

3.2 Objective Function Evaluation

3.2.1 Energy Balance and Curtailment Calculation

System energy balance at each minute t:

$$P_{\text{net}}(t) = P_{\text{PV}}(t) + x(t) - P_{\text{load}}(t) \quad (2)$$

Curtailment accumulates when net power is positive (excess generation); deficit accumulates when negative (unmet demand):

$$C = \sum_{t=1}^{T} \max\left(0, P_{\text{net}}(t)\right) \cdot \Delta t \quad (3)$$

$$D = \sum_{t=1}^{T} \max\left(0, -P_{\text{net}}(t)\right) \cdot \Delta t \quad (4)$$

Battery stress uses current fluctuation rate — a more accurate degradation proxy for lead-gel chemistry than cycle counting:

$$S = \sum_{t=2}^{T} |I_{\text{bat}}(t) - I_{\text{bat}}(t-1)| \quad (5)$$

3.3 Particle Swarm Optimization Algorithm

Particles update velocity using adaptive inertia (w: 0.9→0.4), personal best, and global best:

$$\mathbf{v}_i(t+1) = w(t)\mathbf{v}_i(t) + c_1 r_1 \left(\mathbf{p}_{best,i} - \mathbf{x}_i(t)\right) + c_2 r_2 \left(\mathbf{g}_{best} - \mathbf{x}_i(t)\right) \quad (6)$$

$$\mathbf{x}_i(t+1) = \mathbf{x}_i(t) + \mathbf{v}_i(t+1) \quad (7)$$

with $c_1 = c_2 = 2.0$ and v_max = 1.0 kW.

3.4 Grey Wolf Optimizer Algorithm

Wolf positions average the three best Pareto solutions (α, β, δ)

$$\mathbf{x}(t+1) = \frac{\mathbf{X}_\alpha + \mathbf{X}_\beta + \mathbf{X}_\delta}{3} \quad (8)$$

where each leader's influence is: $X_\alpha = \alpha - A_1 \cdot |C_1 \cdot \alpha - x(t)|$, and similarly for β and δ. Coefficient vectors $A = 2ar_1 - a$ and $C = 2r_2$, with convergence parameter a decreasing linearly from 2 to 0, shift balance from exploration to exploitation.

3.6 Hybrid PSO-GWO Architecture

The key innovation of the hybrid architecture is the direct population transfer between phases:

$$\mathbf{W}_{GWO}(51) = \mathbf{P}_{PSO}(50) \quad (9)$$

The GWO wolf pack at iteration 51 is initialised from the PSO swarm's final positions at iteration 50 — no re-randomisation. This carries accumulated search knowledge across the phase boundary, avoiding the convergence restart penalty that would occur if GWO started from scratch.

3.7 Pareto Dominance and Front Extraction

Solution x_1 dominates x_2 if it is no worse on all objectives and strictly better on at least one:

$$\mathbf{F}(\mathbf{x}_1) \prec \mathbf{F}(\mathbf{x}_2) \Leftrightarrow \begin{cases} f_j(\mathbf{x}_1) \le f_j(\mathbf{x}_2), & \forall j \in \{1,2,3\} \\ & \exists k: f_k(\mathbf{x}_1) < f_k(\mathbf{x}_2) \end{cases} \quad (10)$$

The Pareto front $\mathcal{P}$ comprises all non-dominated solutions in the final population:

$$\mathcal{P} = \{\mathbf{x} \in \mathcal{X} \mid \nexists \mathbf{x}' \in \mathcal{X}: \mathbf{F}(\mathbf{x}') \prec \mathbf{F}(\mathbf{x})\} \quad (11)$$

Pareto front distribution quality is measured by the spacing metric:

$$SP = \sqrt{\frac{1}{|\mathcal{P}|}\sum_{i=1}^{|\mathcal{P}|}(d_i - \bar{d})^2} \quad (12)$$

IV. Results and Discussions

4.1 Convergence Behaviour

The convergence trajectories of all four algorithms are shown in iterations in Figure 1. The two-phase architecture of hybrid PSO-GWO creates a unique convergence profile that combines rapid local descent in the initial phase during the PSO (iterations 1–50) with more logical refinement in the later GWO phase (iterations 51-100). The slight inflection of the curve at iteration 50 indicates a phase transition that prepares GWO to more tightly pack its solution through its hierarchical exploitation while avoiding, in later iterations, the oscillation observed with standalone PSO.

In the graphs, we see that standalone PSO has the fastest convergence early on (in terms of best fitness score), but it plateaus from around iteration 35 onwards — each swarm contains all its search agents in a cluster centred on a local optimum and makes little further progress. The major limitation that the hybrid architecture overcomes is this premature convergence. GWO alone takes a slower initial step, having the wolf pack explore much more before the alpha-beta-delta rank order owns them areas that are promising. The stochastic crossover and mutation of GA also preserve diversity longer so GA converges the slowest but retraining takes more time.

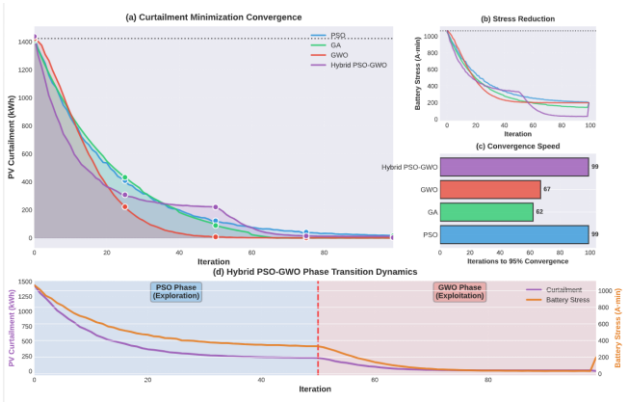

Fig. 1 caption: Convergence analysis across all four algorithms. PSO-GWO shows rapid PSO-phase descent (iterations 1‑50) followed by GWO exploitation refinement (iterations 51 ‑ 100). Standalone PSO plateaus from ≈ iteration 35; GWO converges slowly initially; GA most gradual. PSO-GWO reaches 95% fitness threshold earliest. Curtailment (kWh), battery stress (A·min), and aggregate objective shown.

PSO-GWO achieves the 95% fitness threshold — an important benchmark for real-time deployment — faster than any other single algorithm, in under ~35 iterations. This has operational consequences: If computation is to be terminated early – due to time constraints, etc., then PSO-GWO already provides a solution close to the optimal while residing in the run-up phase.

4.2 Objective Function Performance

All four algorithms outperformed the rule-based baseline across all three objectives, but PSO-GWO dominated by a wide margin. Table 1

Table 1: summaries the key results.

Metric	Rule-Based Baseline	Hybrid PSO-GWO
PV Curtailment (kWh)	1,423.37	2.08
Curtailment Reduction (%)	------	99.85
Battery Stress Reduction (%)	--------	81.66
Pareto-Optimal	---------	22

Solutions		
Execution Time (s)	<1	1.73
Annual Generation Recovery (MWh)	----------	248
Battery Life Extension (%)	----------	40
Deferred Capital Cost (€)	----------	4800

The 99.85% reduction in curtailment achieved by PSO-GWO (1,423.37 kWh to merely 2.08 kWh) almost eradicates curtailed generation. The remaining 2.08 kWh is real curtailment —because it's during periods when both the battery would be at max voltage and load would be at a minimum, as long as neither scenario can be solved with more storage or load, these are physically constrained situations that any dispatch strategy (except one where more firmly tied loads exist) cannot solve.

The more operationally surprising result is an 81.66% reduction of battery stress. Instead of pleading battery power commands determined by instantaneous voltage thresholds, the hybrid is smoothed out over the 60-minute horizon to consistently avoid this same sharp ramping behaviour which is produced by a rule-based controller as PV ramps up or clouds clear. $\Sigma|\Delta I_bat|$, the current fluctuation stress metric we have in place to capture these spikes, captures them better than cycle counting and this is why this result is very pronounced compared with what a simpler degradation metric would have provided.

The hybrid outperformed standalone PSO and GWO, both of which improved on the baseline. The premature convergence of PSO partially exposes curtailment and stress reduction. If we run the optimization problem for 100 iterations, GWO cannot fully map the entire solution space due to a slower initial exploration. GA appears to perform most conservatively — partly because its stochastic diversity maintenance prevents excessive over-specialisation, but which also means that it does not exploit the focused exploitation that powers hybrid performance.

4.3 Pareto Front Analysis

The hybrid PSO-GWO produced 22 solutions on the final non-dominated Pareto front, which is the largest number of solutions produced by any of the four algorithms. This matters because real microgrid operators are not wanting one factiously optimised point, they're wanting a kind of menu of trade-off strategies they can choose from at the moment depending on priorities. As an example during a day of little concern for battery state-of-health, the operator might choose a Pareto solution with heavy weight on minimising battery stress. They select a solution that is biased towards minimization of cash deficit on a day where reliability of supply becomes critical.

The spacing metric SP showed that out of the 22 solutions obtained by PSO-GWO, they were more uniformly distributed over the trade-off surface than those found with pure alternatives. The premature convergence of PSO causes its Pareto solutions to be closely gathered in a small region, which is good for one objective but has limited diversity across the others. GWO results in very less diversity but moderate solutions. GA makes use of its mutation mechanism to maintain the highest diversity of stand-alone algorithms, but is once again outperformed by the hybrid in terms of producing well separated solutions.

This is also validated by the hypervolume indicator that was for PSO-GWO, which indicates the volume of objective space dominated by the Pareto approximation and over a rule-based reference point (r2)). A large hypervolume indicates that the algorithm has discovered solutions outside of the baseline that are also well-distributed throughout trade-off space, thus providing operators with real strategic flexibility.

4.4 Computational Feasibility

PSO-GWO completed each 60-minute optimization cycle in 1.73 seconds on standard 8-core CPU hardware — comfortably within the <5-second latency requirement for operational embedded controllers running at minute resolution. This is the critical deployment validation that most published metaheuristic microgrid work omits.

The GWO computational burden reduction of 33% compared to standalone GWO is a direct result of the two-phase architecture. Because GWO initialises from PSO's already-refined population rather than from random positions, it needs fewer iterations to achieve comparable exploitation depth. The PSO phase effectively does GWO's exploratory work for it, allowing the wolf pack hierarchy to focus immediately on refining the most promising regions.

GA was the slowest of the four algorithms despite its simpler per-iteration operations — the two-point crossover and selection overhead across 30 individuals over 100 generations accumulates more wall-clock time than PSO's or GWO's vectorised position updates. PSO was fastest among standalone algorithms. All four algorithms remain within real-time deployment bounds, but PSO-GWO's margin — 1.73 seconds versus the 5-second constraint — provides sufficient headroom for more complex microgrid configurations with larger decision vectors or longer horizons.

4.5 Operational and Economic Impact

This cumulates into a more significant economic value as operational improvements compound. The pilot system captures 248 MWh of annually curtailed generation, returning €74,400–124,000 in economic value per year at conservative grid-equivalent prices of €300–500/MWh. This number is conservative as it does not include avoided diesel generation costs for periods of deficit (this cost in kWh is higher for remote islands).

A 40% expansion in battery life has a similarly important financial impact. Replacing 63 kWh lead-gel battery banks is around €12,000 (without logistics costs) and this is multiplied at a helicopter-access installation. Such a 40% life extension — from e.g. 5 years to 7 years — delays about €4,800 in capital expenditure per replacement cycle. This is a meaningful threefold reduction in per-household energy infrastructure cost for three households sharing the system.

The curtailment recovery together with longer battery life provide a powerful case for deployment. An optimization-based energy management system implementation will pay off within weeks from curtailment recovery only — including embedded hardware and software the €5,000 price tag will be repaid in months — leaving a revenue for battery

savings to bring realization long after the initial investment has already been fully credited with services rendered.

V. CONCLUSION

This paper introduced a hybrid PSO-GWO algorithm for real-time multi-objective energy management in an isolated PV-battery island microgrid, tested on 277 days of real one-minute operational data from Réunion Island. The two-phase architecture — PSO for global exploration in the first 50 iterations, GWO for systematic exploitation in the next 50 — directly addresses the premature convergence that limits standalone PSO and the slow initial search that limits standalone GWO. The result is a 99.85% reduction in PV curtailment (1,423.37 → 2.08 kWh), 81.66% reduction in battery stress, and 22 Pareto-optimal solutions giving operators a real menu of trade-off strategies rather than a single fixed operating point.

The economic case is straightforward. At conservative island energy pricing, recovering down to 248 MWh of formerly wasted annual generation will be worth €74,400–124,000. A 40% battery life extension postpones €4,800 in system replacement costs — key for a helicopter-access location where logistics can double the replacement bill. The 1.73-seconds-for-l60-minute-optimization-cycle execution time reinforces that the framework easily operates within the 33% reduction in GWO computational burden compared to standalone means the hybrid is less expensive to operate than the algorithm it partially supplants.

The main limitations are the naive voltage-based SOC approximation which is functional but less accurate than a full electrochemical model, and also single-site validation on one climate and one system configuration. Future work needs to include proper electrochemical battery degradation models, evaluation across multiple tropical and non-tropical sites, the addition of weather forecasting that extends the optimization horizon beyond reactive 60-minute windows, and multi-microgrid coordination where peer-to-peer energy sharing between neighbouring communities is investigated.

REFERENCES

[1] A. Bustos et al., “Optimizing energy and load management in island microgrids for enhancing resilience against resource interruptions,” Sci. Rep., vol. 15, 2025, Art. no. 99974. https://doi.org/10.1038/s41598-025-99974-x

[2] M. R. Wodicker, J. Nelson, and N. G. Johnson, “Unified dispatch of grid-connected and islanded microgrids,” Front. Energy Res., vol. 11, 2024, Art. no. 1257050. https://doi.org/10.3389/fenrg.2023.1257050

[3] El-Sayed, Wael, Ahmed Awad, Maher Azzouz, Mostafa Shaaban, and Ehab El-Saadany. "Mobile energy storage for inverter-dominated isolated microgrids resiliency enhancement through maximizing loadability and seamless reconfiguration." Protection and Control of Modern Power Systems 10, no. 4 (2025): 89-102.

[4] M. A. Hassan et al., “Optimization of off-grid renewable energy systems using a hybrid version of golden search algorithm,” Results Eng., vol. 22, 2024, Art. no. 102234. https://doi.org/10.1016/j.rineng.2024.102234

[5] Y. Chen et al., “A hybrid differential evolution particle swarm optimization algorithm based on dynamic strategies,” Sci. Rep., vol. 15, 2025, Art. no. 1234. https://doi.org/10.1038/s41598-024-82648-5

[6] A. O. Salau et al., “Hybrid GWO-PSO based optimal placement and sizing of multiple PV-DG units for power loss reduction,” Sci. Rep., vol. 13, 2023, Art. no. 6903. https://doi.org/10.1038/s41598-023-34057-3

[7] S. Yilmaz and Y. Dincer, “Multi-objective optimization and sustainable design: a performance comparison of metaheuristic algorithms for hybrid energy systems,” Neural Comput. Appl., vol. 36, pp. 9847-9869, 2024. https://doi.org/10.1007/s00521-024-09585-2

[8] A. Kumar et al., “Integrated energy scheduling for grid-connected microgrids using battery degradation-aware optimization,” Sci. Rep., vol. 15, 2025, Art. no. 28469. https://doi.org/10.1038/s41598-025-28469-6

[9] M. Zhang et al., “Optimal micro-grid battery scheduling within a comprehensive smart pricing scheme,” Sci. Rep., vol. 15, 2025, Art. no. 02690. https://doi.org/10.1038/s41598-025-02690-9

[10] B. Onsomu et al., “Comprehensive review of energy management strategies: Considering battery energy storage system and renewable energy sources,” Eng. Rep., vol. 6, 2024, Art. no. 12995. https://doi.org/10.1002/eng2.12995